

Simple Tests for Density Functional Methods

GÁBOR I. CSONKA,¹ NAM ANH NGUYEN,²
ISTVÁN KOLOSSVÁRY³

¹Department of Inorganic Chemistry, Technical University of Budapest, H-1521 Budapest, Hungary

²Laboratoire de Chimie Théorique, Université Laval, Québec, G1 K7P4, Canada

³Department of Chemistry, Columbia University, 410 Havemeyer Hall, New York, New York 10027,

Received 22 January 1997; accepted 20 March 1997

ABSTRACT: The performance of the currently used generalized gradient approximation density functionals is analyzed using several simple, yet critical requirements. We analyze the effects of the self-interaction error, the inclusion of the exact exchange, and the parameter settings used in the popular three-parameter hybrid density functionals. The results show that the elimination of the self-interaction error from the current density functionals lead to very poor results for H₂. The inclusion of the exact exchange does not significantly influence the self-interaction corrected results. The variation of the *A*, *B*, and *C* parameters of a hybrid DFT method influences the H—H equilibrium bond length through a very simple linear equation, and it is possible to reproduce the experimental H—H distance with appropriate selection of these parameters, although an infinite number of solutions exists. Similar results were obtained for the total energy and the electron density along the internuclear axis. The analysis of the exact KS potential at the bond critical point of the dissociating H₂ molecule shows that, for this property, the second order Moller–Plesset perturbation theory yields a better potential than the density functionals studied in this article. © 1997 John Wiley & Sons, Inc. *J Comput Chem* 18: 1534–1545, 1997

Keywords: self-interaction error; hybrid functionals; H₂, total energy; equilibrium bond length; electron density; KS potential

Correspondence to: G. I. Csonka; e-mail: csonka@web.inc.bme.hu

Contract/grant sponsor: Hungarian Research Foundation; contract/grant numbers: OTKA T16328, T14247.

Introduction

Kohn and Sham¹ proved that the exact ground-state electron density and energy of a many-electron system may be obtained by solving self-consistent field (SCF) equations analogously to the Hartree–Fock (HF) method. In the Kohn–Sham (KS) method, the HF exchange energy is replaced by the exchange correlation energy, which is a functional of the electron density, and the HF exchange potential is replaced by the exchange correlation potential (i.e. the KS potential), which is the functional derivative of the exchange correlation energy.^{2,3} KS formalism can be implemented similarly to the HF method, thus the computational cost of KS DFT is similar to that of the HF method. The exact self-consistent KS equations¹ yield eigenfunctions, ϕ_j , and eigenvalues, ε_j , in the same way as the HF method. Moreover, the KS ϕ_j orbitals reflect the correlation effects and yield the exact electron density, $\rho(r)$, and the KS highest eigenvalue, $\varepsilon_{\text{HOMO}}$, is the negative of the exact, many-body ionization potential.

The exact KS exchange term can be calculated from the ϕ_j orbitals. However, the exact Coulomb correlation potentials are generally not known, consequently, approximate potentials are used in practice. The most successful generalized gradient approximation (GGA) DFT methods^{4–7} use a unified derivation of the exchange and correlation terms. It should be noted that the exchange and correlation energy, as defined in DFT, may be different from the conventional exchange and correlation energy (i.e. with respect to the HF method as reference).⁸ It was also observed that, because of cancellation effects, the results are better if the exchange and correlation terms are approximated together⁹ compared with the results obtained with the exact exchange.^{10–13} The GGA DFT provides a very efficient recovery of electron correlation compared with very expensive traditional methods and yields quite good thermochemistry in the standard thermochemical test set of molecules.¹⁴

The studies of GGA exchange correlation holes and the adiabatic connection formula¹⁵ have shown that the exact exchange hole is poorly represented by GGA models in covalent bonds.^{16,17} To remedy this error, a simple, three-parameter hybrid GGA model was proposed and the exact exchange was mixed with the GGA functionals. The weight of the exact exchange and local approximation was

chosen to fit the experimental thermochemical data.¹⁶ The proposed mixing reduced the 6-kcal/mol average atomization energy errors of GGA to 2.4 kcal/mol in the same thermochemical test set of molecules.¹⁶ In 1995, Becke constructed a new correlation functional (termed Bc95) on the basis of four exact conditions (uniform electron gas limit, distinct treatment of opposite-spin and parallel-spin correlations, self-interaction free, and fitted to exact correlation energies of atoms).¹⁷ This new correlation functional did not perform particularly well when combined with Becke's earlier exchange functional (termed B). The average and maximum errors were 8.6 kcal/mol and 28.6 kcal/mol, respectively; however, one parameter inclusion of the exact exchange reduced these errors to 2.0 and 7.5 kcal/mol, respectively.¹⁷

An alternative method for development of functionals is presented by Perdew's group. Graphical comparison of the enhancement factors over local exchange permits the analysis of errors of different GGAs.¹⁸ These diagrams help to check the existing functionals if they satisfy the exact known conditions for the exchange correlation hole. It has been shown that neither of the currently used functionals satisfy all known conditions. For example, the low-density convexity constraint provides a difficult challenge for approximate functionals to meet. Fortunately, this is not an important condition for most real systems, which are very far from the low-density limit.

The essential problem is that the GGA form is too simple to represent all of the nonlocality of exchange correlation (no matter which exact conditions we impose upon it). "The residual GGA error is just the price we pay for having a simple, easily implemented, universal functional. The GGA form is most appropriate for uniform or slowly varying densities. When we apply it to molecules or atoms, we are extrapolating."¹⁹ The Perdew–Wang (PW) correlation functional^{20,21} was designed to satisfy as many conditions as possible and it satisfies more exact conditions than the Perdew (P) functional. However, the two functionals show similar performance (the PW functional is more reliable for difficult cases).²² Moreover, the Lee–Yang–Parr (LYP) functional,⁷ which is inaccurate in the uniform electron gas limit¹⁸ and incorrectly gives zero correlation energy in any ferromagnetic (all spins aligned) system, frequently yields good results with chemical examples. To illustrate the difficulties further we recall that the improved bond energies of Becke's exchange functional was attributed to the better asymptotic be-

havior to the exchange energy density.⁶ Later, Engle et al. showed that Becke's exchange energy density attains the correct behavior at large distances where it has almost no effect on the energy.²³ These investigators constructed a functional that did not satisfy the correct asymptotic condition but yielded even better exchange energies. Further study showed that the GGA corrections provided much improvement in energies over the LSDA; however, they provide much less improvement in asymptotic behavior of the exchange correlation potential.²⁴ An indication of this is that the GGA potentials provide almost no improvement in LSDA eigenvalues, which are generally seriously in error.

Another source of error is the self-interaction error. In exact KS theory, a Coulomb self-interaction contribution is exactly canceled by an exchange contribution (like in HF theory) and the correlation self-interaction contribution is zero. Approximate exchange correlation functionals result in an imperfect cancellation of the Coulomb and exchange terms and nonzero correlation self-interaction contributions. To remedy this, Perdew and Zunger²⁵ proposed an orbital-based self-interaction correction (SIC) for atoms at the LSDA level. We previously mentioned that Becke proposed a self-interaction free correlation functional, Bc95. The comparison of atomization energy data shows that B-Bc95 exchange correlation combination is inferior to Becke or PW in thermochemical examples,¹⁷ despite the self-interaction error of the PW functional. Recent investigations of the self-interaction error showed that this error is more important for hydrogen abstraction barriers than for heat of formations²⁶ and the primary source of this error is in the Coulomb-exchange part.²⁷ Thus, eliminating the self-interaction for a correlation functional alone will not improve the results. We mention that the LYP correlation functional is also self-interaction-free; however, the Becke or LYP methods provide a considerable self-interaction error for hydrogen abstraction barriers.^{26,27}

Buijse et al. constructed an exact KS potential from the electron density of two-electron systems.²⁸ They have shown that the LSDA + Becke-Perdew GGA has a different functional dependence on the electron density than that of the exact KS potential.²⁹ It should be noted that the difference may integrate close to zero, thus approximate GGA DFT functionals provide reasonable energetic results. They have also proposed an iterative procedure to construct accurate exchange correlation potentials for many-electron systems from the

ground state electron density, $\rho(\mathbf{r})$.²⁸ A similar procedure was proposed by Wang and Parr.³⁰ The ground state electron densities and first and second order density matrices obtained from full configuration interaction (CI) calculations were recently used to construct correlation energy densities for the He atom and H₂ molecule.³¹ Also, recently, Burke et al. proposed an approach to obtain accurate energies from exact electron densities.³² Comparisons of the electron densities calculated by various methods provided some interesting insights into the working mechanism of the electron correlation.³³

In the present work the functional dependence of the equilibrium molecular geometry and total energy of H₂ is analyzed. We pay a special attention to the self-interaction error and the influence of the *A*, *B*, and *C* parameters of the hybrid functionals, thus the inclusion of the exact exchange. Next, we analyze the exact KS potential in the bond critical point of the dissociating H₂ molecule. Finally, we analyze the functional dependence of the errors of the electron density along the internuclear axis in H₂. The errors in the DFT exchange correlation functionals manifest themselves through incorrect ground state electron density distributions. Provided that the exact electron density or a very good (preferably full CI) approximation for the exact electron density is known, we can compare it to various approximate electron density distributions, $\rho(\mathbf{r})$. The gradient vector field, $\nabla\rho(\mathbf{r})$, and the Laplacian, $\nabla^2\rho(\mathbf{r})$, of the electron density can also be used for comparison purposes. The H₂ molecule is suitable for this study, because the complete CI results can be approached. The H₂ molecule is also the simplest existing molecule in which the exchange correlation effects can be studied. The exact KS potential of H₂ can be easily expressed in terms of $\rho(\mathbf{r})$, $|\nabla\rho(\mathbf{r})|$, and $\nabla^2\rho(\mathbf{r})$.

Computational Methods

The Kohn-Sham¹ total energy (E_{KS}) is composed from the following energy terms:

$$E_{KS} = E_T + E_V + E_J + E_X + E_C \quad (1)$$

where E_T is the noninteracting kinetic energy, E_V is electron-nuclear attraction energy, E_J is the electron-electron Coulomb repulsion energy, E_X is exchange energy, and E_C is the correlation energy. The SIC²⁵ was designed to fulfill the follow-

ing equations for any one electron density, $\rho_1(\mathbf{r})$:

$$E_X[\rho_1(\mathbf{r}), 0] = -E_J[\rho_1(\mathbf{r})] \quad (2)$$

$$E_C[\rho_1(\mathbf{r}), 0] = 0 \quad (3)$$

where 0 in the bracket is the opposite-spin electron density.

The following self-interaction correction term is added to the energy:

$$E_{SIC} = - \sum_i (E_J^i + E_X^i + E_C^i) \quad (4)$$

where

$$E_J^i = \frac{1}{2} \iint \rho_i(\mathbf{r}_1) \frac{1}{r_{12}} \rho_i(\mathbf{r}_2) d\mathbf{r}_1 d\mathbf{r}_2 \quad (5)$$

$$E_X^i = \int F_X[\rho_i(\mathbf{r}), 0] dr \quad (6)$$

$$E_C^i = \int F_C[\rho_i(\mathbf{r}), 0] dr \quad (7)$$

where the summation is running over all occupied orbitals; ψ_i , F_X , and F_C are exchange and correlation functionals, respectively; and $\rho_i(\mathbf{r}) = |\psi_i|^2$.

It should be noted that the orbitals that minimize the SIC total energy are not the KS orbitals. These orbitals are localized and elaborate methods are required to construct them for larger molecules. For SIC calculations we used the program described in Refs. 26 and 27.

We use the following combinations of functionals:

- (i) **B-P** and **B-PW**: The Becke 88 exchange function⁶ is combined with the correlation functionals of Perdew 86⁵ and Perdew-Wang 91,²⁰ respectively.
- (ii) **B3P** is a hybrid method. It is a linear combination of various exchange and correlation functionals in the form:

$$\begin{aligned} A \cdot E_X[\text{Exact}] + (1 - A) \cdot E_X[S] \\ + B \cdot \Delta E_X[B] + E_C[\text{VWN5}] \\ + C \cdot \Delta E_C[P] \end{aligned} \quad (8)$$

where $E_X[\text{Exact}]$, $E_X[S]$, and $\Delta E_X[B]$ are the exact, Slater, and Becke⁶ exchange functionals and $E_C[\text{VWN}]$ and $\Delta E_C[P]$ are the Vosko, Wilk, and Nussair 5³⁴ and Perdew⁵ correlation functionals, respectively. Note that $\Delta E_X[B]$ is a gradient correction to the S + VWN or LSDA, for exchange,

and $\Delta E_C[P86]$ is a gradient correction for correlation.

The constants A , B , and C are those determined by Becke by fitting heats of formation ($A = 0.2$, $B = 0.72$, $C = 0.81$).¹⁶ Note that Becke used the PW correlation functional instead of P.¹⁶

- (iii) **P-LYP** method, in which Becke's exchange functional is combined with the correlation functional of Lee, Yang, and Parr.⁷
- (iv) **B3LYP** is a hybrid method. This functional was not published before the implementation into the Gaussian-92/DFT.³⁵ It is a logical extension of Becke's three-parameter concept using different correction functionals (e.g., LYP) in the form:

$$\begin{aligned} A \cdot E_X[\text{Exact}] + (1 - A) \cdot E_X[S] \\ + B \cdot E_X[B] + (1 - C) \\ \cdot E_C[\text{VWN3}] + C \cdot E_C[\text{LYP}] \end{aligned} \quad (9)$$

The constants A , B , and C are selected to be equal to those determined by Becke for the B3P method. Note also that different VWN parameterized is used for the local correlation.

The calculations were carried out using the Gaussian-94³⁶ computer program on Silicon Graphics workstations. A fine-pruned grid having 75 radial shells and 302 angular points per shell (about 7000 points per atom) was used in all calculations. For comparison, we also calculated the electron density with HF, CISD, and correlated single reference many-body perturbation theory (MBPT) using Møller-Plesset partition³⁷ to the second order (MP2). The geometry of the hydrogen molecule was fully optimized using various methods supplemented with triple-split-valence plus polarization 6-311G(d, p), (d, 2pd), and (d, 3pd)³⁸ basis sets. The properties of the gradient vector field of the electron density, $\nabla\rho(\mathbf{r})$, were calculated from the wave functions prepared by the Gaussian using the AIMPAC package,³⁹ which was modified in our laboratory to perform grid calculations.

Results and Discussion

GEOMETRIES

Figure 1 shows the equilibrium H—H distance for the H₂ molecule vs. theoretical methods sup-

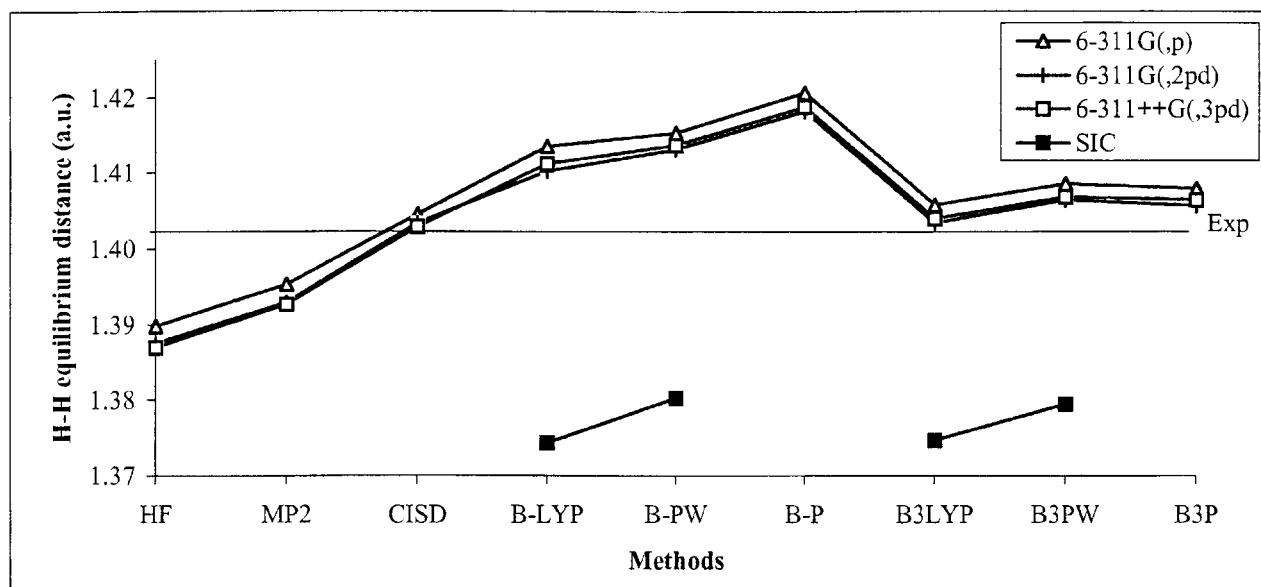


FIGURE 1. Optimized H—H distances of H_2 equilibrium structure. SIC denotes the DFT calculations with self-interaction correction and 6-311++ G(d,3pd) basis set. The experimental result is denoted by a horizontal line.

plemented with 6-311G(d,p), 6-311G(d,2pd), and 6-311++ G(d,3pd) basis sets. The CISD results (CISD is full CI for the H_2 molecule) show the smallest basis set dependence and they are very close to the experimental results. The HF results show a characteristic bond shortening for the H—H covalent bond. The origin of this bond shortening will be discussed later. The inclusion of the Coulomb correlation provides considerable bond lengthening. The Coulomb correlation introduced by the MP2 method is quite insufficient as the MP2 results are closer to HF than CISD results (cf. Fig. 1).

The LSDA H—H equilibrium bond length is very long (1.45 Bohr; not shown in Fig. 1). The GGA DFT methods provide considerably better, although overly long, equilibrium distances. The B-PW functional performs better than the B-P for H_2 and H_3 (cf. Fig. 1 and Refs. 26 and 40). Slightly better agreement with CISD results was obtained with B-LYP functional. The partial inclusion of the exact exchange (B3LYP, B3PW, and B3P in Fig. 1) provide very close results to CISD and experiment. At first sight it might be said that the GGA DFT methods exaggerate the Coulomb correlation effects and the inclusion of the exact exchange dampen this overcorrelation. However, it should be noted that these functionals are not self-interaction-free and the introduction of self-interaction correction (SIC) results in large effects.²⁷ It was observed that the SIC shortens the H_2 bond length

by 0.03–0.04 Bohr, thus the GGA DFT + SIC calculations provide too-short H_2 bond lengths (cf. Fig. 1 and Refs. 26 and 27). It is interesting to note that the GGA + SIC H_2 bond lengths are shorter than the HF bond lengths, thus the main source of the bond lengthening for H_2 is the self-interaction error that simulates the Coulomb correlation effects for H_2 . The inclusion of the exact exchange does not significantly influence the SIC results. It should also be noted that the effect of the inclusion of SIC is larger than the inclusion of the exact exchange (cf. Fig. 1).

The GGA DFT and hybrid DFT H_2 equilibrium bond lengths do not show large basis set dependence. The 6-311G basis set provides fairly stable results, only a -0.0022 -Bohr bond shortening was experienced as the basis set quality was increased from (d,p) to (d,2pd). This is similar to the corresponding HF (-0.0022 Bohr), MP2 (-0.0024 Bohr), and CISD (-0.0011 Bohr) basis set extension effects. All methods are consistent in bond shortening as the basis set quality increases, the largest basis set effect was shown with the BLYP method (-0.0033 Bohr) (cf. Fig. 1). A recent investigation of the DFT basis set extension effects yielded similar results.⁴¹ The improvement of the basis set to 6-311++ G(d,3pd) results in a fairly small bond distance change (it is below -0.0004 Bohr).

To study the inclusion of exact exchange we varied the A , B , and C coefficients of Eq. (8) over the ranges 0.1–0.4, 0.65–0.75, and 0.75–0.95, re-

spectively, and calculated the corresponding B3P/6-311G(d,2pd) H₂ equilibrium bond length. These calculations yielded the following equation:

$$r(\text{H—H}) = 1.4413 - 0.0860 \cdot A - 0.0500 \cdot B + 0.0220 \cdot C \text{ (Bohr)} \quad (10)$$

This equation provides very precise (up to four decimal places) H₂ bond lengths, $r(\text{H—H})$ in the given range. The predictive force of this simple equation is quite surprising and signals that these effects are independent of each other in the parameter range studied. As expected, the increasing weight of the exact exchange shortens the bond length. Becke's gradient correction for exchange decreases, and Perdew's gradient correction for correlation increases H—H bond length. It is possible to reproduce the experimental (1.401 Bohr) H—H distance with appropriate selection A , B , and C . It should be noted that an infinite number of solutions exist that reproduce the experimental bond length.

A rather similar equation was obtained for the B3P/6-311G(d,p) results:

$$r(\text{H—H}) = 1.4437 - 0.0860 \cdot A - 0.0500 \cdot B + 0.0220 \cdot C \text{ (Bohr)} \quad (11)$$

thus, apart the slightly larger $r(\text{H—H})$, the coefficients of eqs. (10) and (11) agree with each other. The B and C parameters cancel each other's effect, thus these parameters seem somewhat superfluous. This is in accordance with recent results of

Perdew's group⁴² and with the latest hybrid functional proposed by Becke.¹⁷

TOTAL ENERGY

Table I shows the total energies for H₂ molecule using various levels of theory. It should be noted that, except for the BLYP method, the GGA DFT methods provide slightly lower energies (italic values in Table I) than the experimental value. The only exception is the B3P method, which provides considerably lower energy (cf. Fig. 2). The basis set effects are smaller for the GGA DFT methods than for MP2 or CISD methods. It seems that the GGA DFT methods recover the Coulomb correlation energy even with relatively small basis sets. Improving the basis set quality from 6-311G(d,2pd) to the 6-311++ G(d,3pd) level results in only about a 0.02-millihartree energy decrease (Table I). This small energy decrease is up to 10 times smaller than basis set effects of CISD or MP2 methods. However, it should be noted that the inclusion of SIC considerably changes the PW energies, whereas it has quite an insignificant effect on LYP energies. The origin of the too-low energies is the electron self-interaction error.

We varied the A , B , and C coefficients of eq. (8) over the ranges of 0.05–0.4, 0.65–0.75, and 0.75–0.95, respectively, and calculated the corresponding B3P/6-311G(d,2pd) total energies. These calculations yielded the following equation:

$$E(\text{tot}) = -1.17213 - 0.0908 \cdot A - 0.0892 \cdot B + 0.0481 \cdot C \quad (12)$$

TABLE I. Total Basis Set Extension and SIC Energies (a.u.) for H₂ Molecule Calculated with Various Methods and Basis Sets.^a

Method	6-311G(d, p)	6-311G(d, 2pd)	6-311++ G(d, 3pd)	$\Delta E(2pd)$	$\Delta E(+3pd)$	$\Delta E(\text{SIC})^b$
HF	–1.13249	–1.13300	–1.13307	–0.00051	–0.00007	
MP2	–1.16027	–1.16463	–1.16495	–0.00436	–0.00032	
CISD	–1.16834	–1.17231	–1.17253	–0.00397	–0.00022	
B–LYP	–1.16917	–1.16961	–1.16962	–0.00044	–0.00001	–0.00061
B–PW	–1.17616	–1.17650	–1.17651	–0.00035	–0.00001	0.01316
B–P	–1.17752	–1.17789	–1.17791	–0.00037	–0.00002	
B3LYP	–1.17957	–1.18001	–1.18003	–0.00044	–0.00002	0.00039
B3PW	–1.17858	–1.17895	–1.17897	–0.00037	–0.00002	0.01187
B3P	–1.21515	–1.21555	–1.21558	–0.00040	–0.00003	

^a Energies lower than experiment (–1.1744 a.u.) are in italic. $\Delta E(2pd)$ is the energy change between (d, p) and (d, 2pd) basis sets, $\Delta E(+3pd)$ is the energy change between (d, 2pd) and ++ G(d, 3pd) basis sets.

^b From Ref. 27. The SIC was calculated with the 6-311++ G(d, 3pd) basis set.

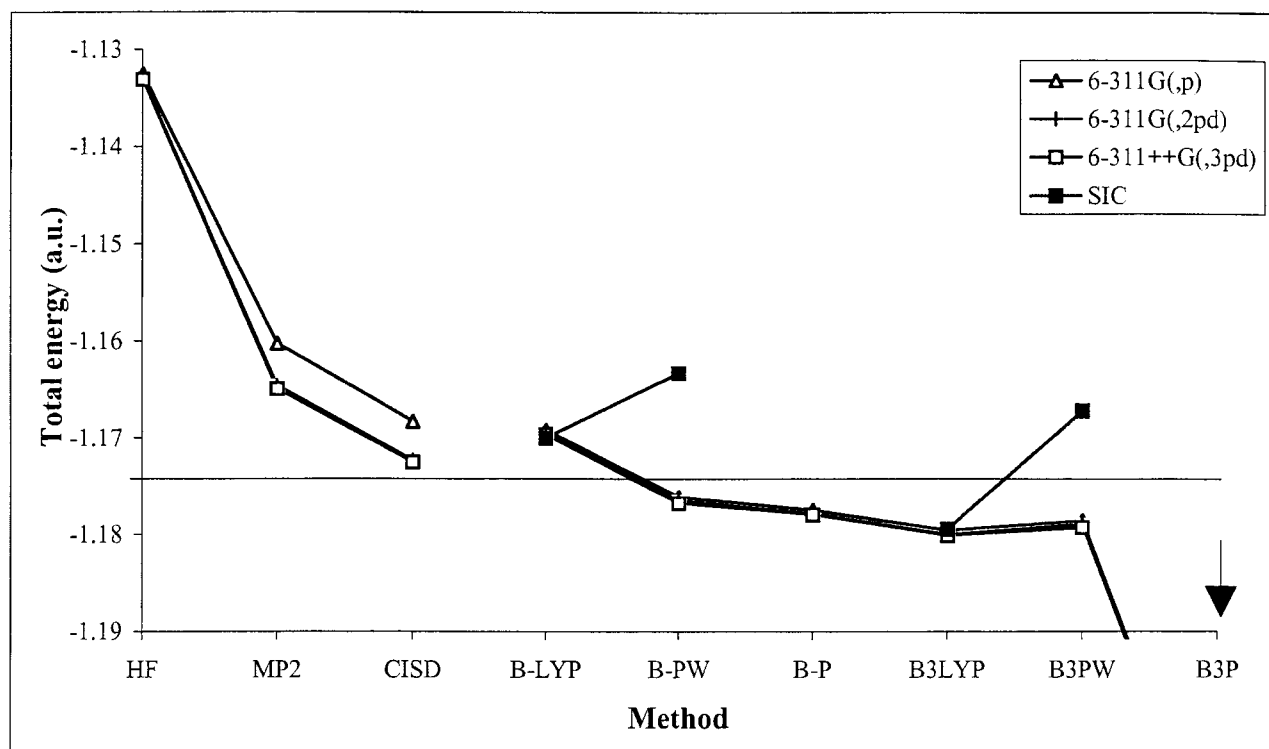


FIGURE 2. The calculated total energies of the H_2 equilibrium structure. SIC denotes the DFT calculations with self-interaction correction and 6-311++ G(d, 3pd) basis set. The CISD result is denoted by a horizontal line. The extremely low energy (less than -1.2155 a.u.) provided by B3P method is shown by the arrow.

The energies calculated by the help of this equation usually show a rather good agreement (within 0.02 millihartree) with the real hybrid DFT results. If $A > 0.3$, then the precision of the approximation becomes worse. At $A = 0.4$ the error is about 0.14 millihartree. A rather similar equation was obtained for the B3P/6-311G(d, p) results:

$$E(\text{tot}) = -1.17175 - 0.0908 \cdot A - 0.0892 \cdot B + 0.0481 \cdot C \quad (13)$$

This equation again provides quite good agreement with the computed hybrid DFT results. The observations made above for the H_2 equilibrium bond length are valid for the energy. For example, the appropriate selection of the B and C parameters (C is equal to about 2 B) cancel each other's effect.

EXACT KS POTENTIAL IN BOND CRITICAL POINT

The occupied KS orbital, $\psi(\mathbf{r})$, of the ground state of the H_2 molecule can be expressed by the electron density [$\psi(\mathbf{r}) = \sqrt{\rho(\mathbf{r})/2}$]. Introducing this into the KS equations provides an explicit

expression for the exact KS potential of H_2 , v^{KS} :⁴³

$$v^{KS}(\mathbf{r}) = \frac{\nabla^2 \rho(\mathbf{r})}{4\rho(\mathbf{r})} - \frac{(\nabla \rho(\mathbf{r}))^2}{8\rho(\mathbf{r})} + \varepsilon \quad (14)$$

where $\rho(\mathbf{r})$ is the exact ground state electron density and ε is the ionization potential of the hydrogen molecule. In the bond critical point (BCP), the $\nabla \rho(\text{BCP}) = 0$; thus:

$$v^{KS}(\text{BCP}) = \frac{\nabla^2 \rho(\text{BCP})}{4\rho(\text{BCP})} + \varepsilon \quad (15)$$

It is known that the description of the dissociation of the H_2 molecule is a thorough test for any method. Leeuwen and Baerends have shown that GGA DFT potentials fail to provide correct behavior of the potential in the BCP.⁴² These approximate potentials go to infinity as the H_2 molecule is dissociating, while the exact $v^{KS}(\text{BCP})$ goes to the positive constant, $-\varepsilon$.³⁷ Figure 3a shows the CISD/6-311G(d, 2pd) Laplacian in the bond midpoint (BCP) as a function of H—H distance below 5 Bohrs. It is expected that the Laplacian values decay exponentially at large H—H distances. Figure 3a clearly shows that, below 5 Bohrs, the

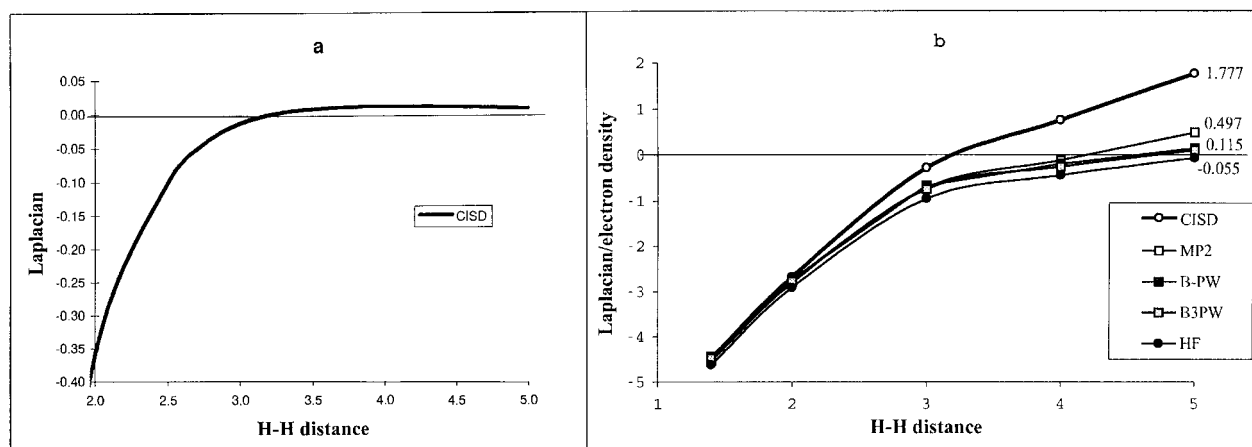


FIGURE 3. The Cisd Laplacian (BCP) (a) and the method dependence of Laplacian (BCP) / density (BCP) (b) vs. the H—H distance in the dissociating H_2 molecule. BCP denotes the bond critical point (the midpoint). The calculations were carried out with the 6-311G(d, 2pd) basis set.

$\nabla^2\rho(\text{BCP})$ has not reached yet its exponentially decaying range, while the electron density in the bond midpoint, $\rho(\text{BCP}, R_{\text{HH}})$, decays exponentially above the 3.5-Bohr H—H distance. The following equation was thus obtained:

$$\rho(\text{BCP}, R_{\text{HH}}) = 1.451 e^{-1.1317 R_{\text{HH}}} \quad (16)$$

in atomic units. Thus, $\nabla^2\rho(\text{BCP})/\rho(\text{BCP})$ in Figure 3b is far from being constant. Because of the convergence problems with Gaussian-94 for Cisd calculations above the 5-Bohr interatomic distance we could not calculate addition points. Another limiting factor may be the use of Gaussian basis sets, as they are not completely reliable asymptotically. The curves below 5 Bohrs in Figure 3b clearly show that, at a normal covalent bond length, the Cisd potential is approximated quite well in the BCP by any of the potentials calculated from HF, DFT, or MP2 electron density; however, above 3 Bohrs, the error becomes quite important. The poor performance of the HF method is apparent, and the GGA DFT functionals show only very slight improvement. At large internuclear separation the MP2 method provides a considerably better potential than the DFT methods studied here.

ELECTRON DENSITY ALONG THE BOND PATH

Besides comparison of the calculated electron densities and Laplacians in the BCP, comparison of the electron densities along the internuclear axis can reveal further details. We do not consider our values for electron density to be completely pre-

cise very near the nuclei or asymptotically because our densities are represented in terms of Gaussian basis sets. Figure 4a shows the electron density differences calculated by various methods compared with Cisd results for the geometry-optimized H_2 . Figure 4b shows the electron density differences for a fixed, 1.401-Bohr H_2 distance. The origin of the horizontal coordinate is placed in the BCP in these figures and the largest distance is 1.3 Bohrs, thus these curves should be free of asymptotic errors. Comparison of Figure 4a and b reveals that the geometry optimization influences the $\rho(\text{BCP})$ considerably. All methods, except LSDA, approximate the Cisd electron density in the BCP within 0.002 a.u. for a fixed H_2 distance (cf. Fig. 4b). The geometry optimization nearly triples those differences and produces step-like difference functions near the nuclei. Figure 4a and b clearly show that the HF method overconcentrates the electron density for covalent bonds in the BCP, while a serious underestimation of the electron density occurs near the nuclei. This necessarily results in too-short covalent bond lengths (cf. "Geometries" subsection), and in an overestimation of the electron density in directions perpendicular to the bond axis. The MP2 method improves the electron density considerably. The poor performance of the B-LYP functional is apparent from Figure 4a and b. It provides the opposite error as compared with the HF method—a small electron density in the BCP and an overestimated electron density near the nuclei. The B-P method provides a considerably better electron density than the B-LYP, whereas the B-PW is slightly worse than the B-P

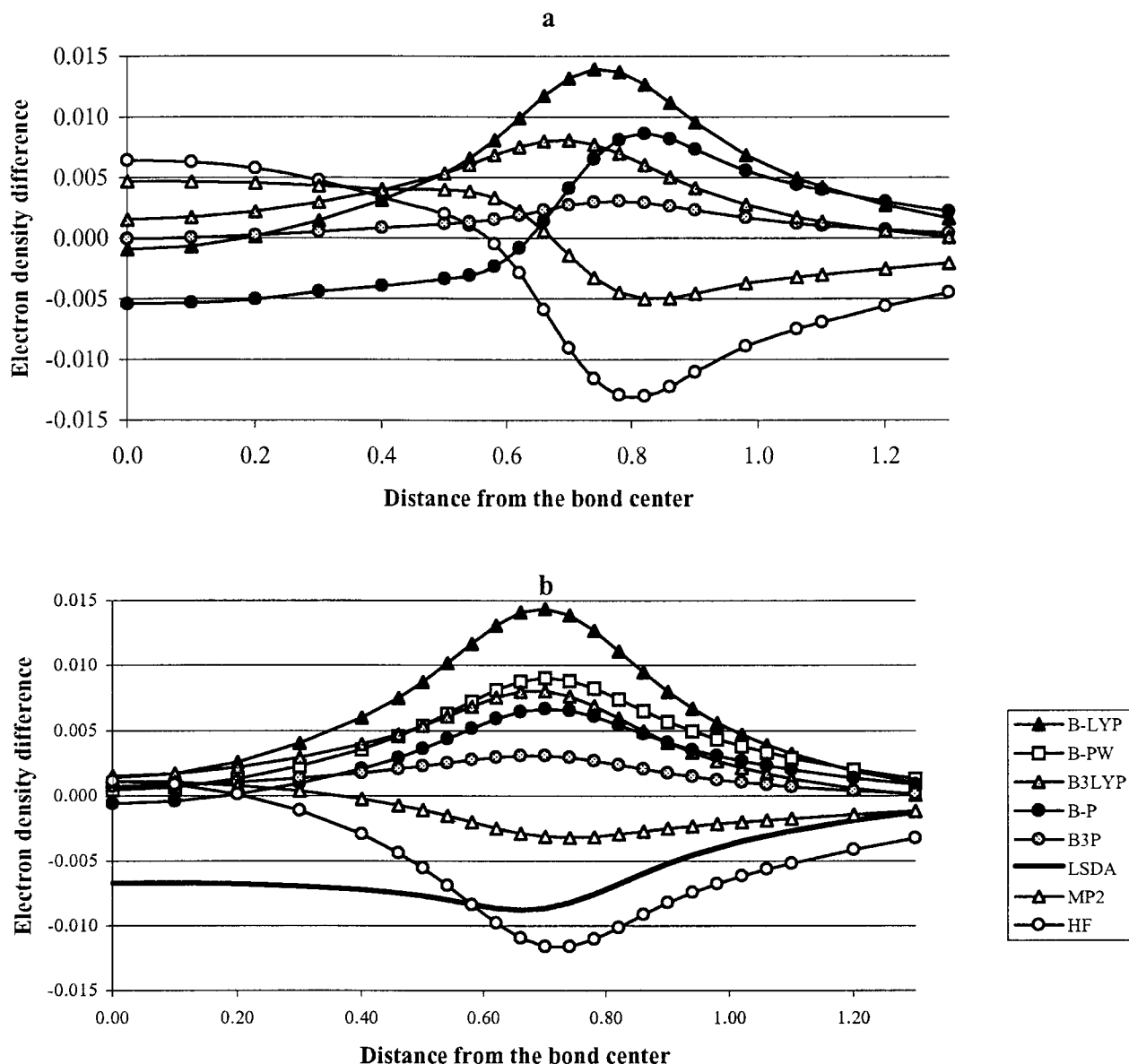


FIGURE 4. Electron density differences (a.u.) as a function of the distance (Bohrs) from the bond center in H_2 along the internuclear axis calculated at optimized (a) and experimental (b) H_2 distances. The CISD/6-311G(d, 2pd) electron density was used as a reference. Negative values indicate smaller electron densities compared with CISD results.

method. The B3P method yields the best agreement with CISD electron density for H_2 .

This fact inspired us to test the influence of the A , B , and C parameters of eq. (8) on the electron density of H_2 at experimental interatomic distance. Figure 5 shows that it is possible to obtain a nearly perfect agreement with the CISD/6-311G(d, 2pd) electron density and we were able to reduce the electron density difference below ± 0.0003 a.u. along the internuclear axis. However, for this purpose, the originally proposed A , B , and C parameters should be changed. The slight

increase of A to 0.21 seems to be necessary to get correct electron density in the BCP. The values of B and C parameters of eq. (8) play an important role. The $B = 0.72$ and $C = 0.81$ values are responsible for the too large electron density peak in the nuclei for the B3P method. Setting the value of C to 0.91 and the value of B to 0.67 eliminates most of this peak. It is interesting to note that the parameter values of B and C of eq. (8) influence the electron density near the nuclei, whereas the value of A influences the electron density mainly in the BCP. The parameters B and C again act in

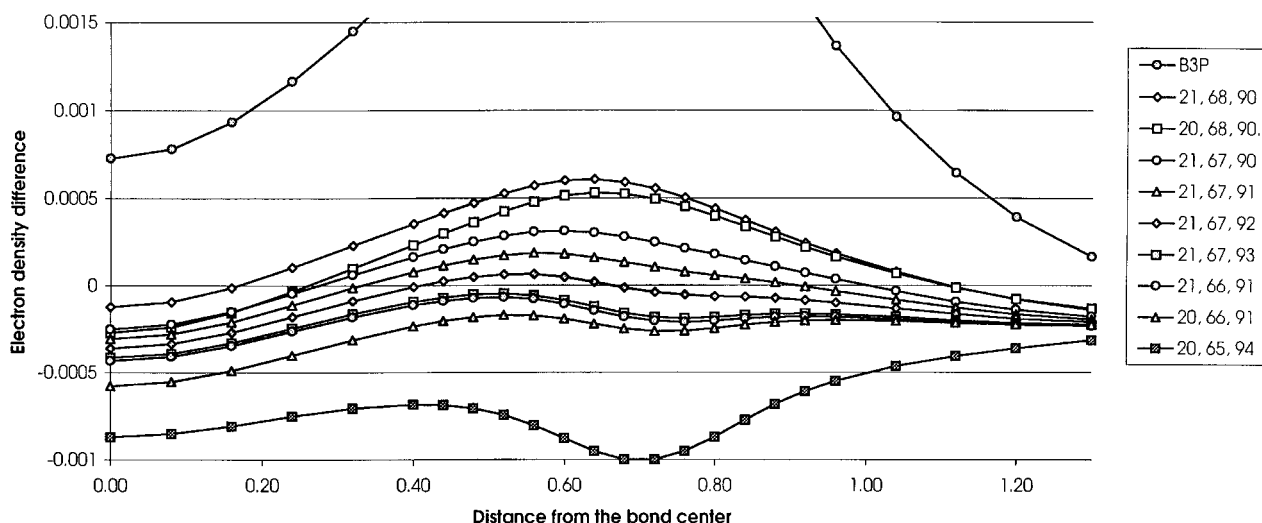


FIGURE 5. Electron density differences (a.u.) calculated at an experimental H_2 distance as a function of the distance (Bohrs) from the bond center in H_2 along the internuclear axis. The CISD / 6-311G(d, 2pd) electron density was used as a reference. Negative values indicate smaller electron densities compared with CISD results. The legend shows 100-fold values of A , B , and C . Numbers 21, 68, 90 indicate $A = 0.21$, $B = 0.67$, and $C = 0.91$ in eq. (1).

the opposite direction: a one-point decrease in B has the effect of a two-point increase in C (cf. Fig. 5).

Conclusions

It has been shown that GGA DFT methods provide too-long equilibrium distances for H_2 ; however, the partial inclusion of the exact exchange provides very close results to CISD and experiment. The main source of the bond lengthening is the self-interaction error that simulates the Coulomb correlation effects for H_2 . The inclusion of the exact exchange does not significantly influence the self-interaction corrected results and it results in a much smaller effect than the self-interaction.

The values of A , B , and C parameters of the B3P hybrid DFT method influence the H—H equilibrium bond length through a very simple linear equation [cf. eqs. (10) and (11)]. The increasing weight of the exact exchange shortens the bond length. Becke's gradient correction for the exchange shortens the H—H bond, and Perdew's gradient correction for the correlation lengthens the H—H bond. It is possible to reproduce the experimental H—H distance with appropriate selection of A , B , and C parameters. It should be noted that an infinite number of solutions exist and the B and C parameters may cancel each other's effects as they act in the opposite direction.

The GGA DFT methods provide slightly lower energies than the experimental value for H_2 . The origin of the too-low energies is the electron self-interaction error. The basis set effects are up to 10 times smaller for the GGA DFT methods than for MP2 or CISD methods.

The values of A , B , and C parameters of the B3P hybrid DFT method influence the total energy of H_2 through a very simple linear equation [cf. eqs. (12) and (13)]. The increasing weight of the exact exchange (A) and Becke's gradient correction for the exchange (B) decrease, and the increasing weight of Perdew's gradient correction for the correlation (C) increases the total energy. The appropriate selection of the B and C parameters cancels out each other's energetic effect.

From the study of electron density and the Laplacian of the electron density in the bond critical point of the dissociating H_2 molecule the following conclusion can be drawn: The GGA DFT functionals show only a very slight improvement over the HF method. At large internuclear separation the MP2 method provides a considerably better potential than the DFT methods studied here.

Investigation of the electron densities along the internuclear axis reveal the typical HF error for covalent bonds. The HF method overconcentrates the electron density in the bond critical point while a serious underestimation of the electron density occurs near the nuclei. The GGA DFT methods provide the opposite error.

The suitable selection of the A , B , and C parameters of the B3P-type hybrid functional resulted in a nearly perfect agreement (electron density difference below ± 0.0003 a.u.) with the full CI electron density along the internuclear axis. The originally proposed A , B , and C parameters provide a large electron density peak in the nucleus for the B3P method. The parameter values of B and C influence the electron density near the nuclei, while the value of A influences the electron density, mainly in the BCP. A slight increase of A to at least 0.21 seems necessary to obtain correct electron density in the BCP. $B = 0.67$ and $C = 0.91$ eliminates nearly completely the error of the electron density near the nuclei. The parameters B and C again compensate each other's effect: a 1% decrease in B has the effect of a 2% increase in C .

Acknowledgments

We are grateful to Professor John P. Perdew for helpful discussions and for reading the manuscript. G.I.C. acknowledges the PAST professorship provided by the French Government, and the kind hospitality of Professor J.-L. Rivail. The financial support of the Hungarian Research Foundation (OTKA T16328 and T14247) is acknowledged.

References

1. W. Kohn and L. Sham, *J. Phys. Rev. A*, **140**, 1133 (1965).
2. R. G. Parr and W. Yang, *Density Functional Theory of Atoms and Molecules*, Oxford, New York, 1989.
3. R. M. Dreizler and E. K. U. Gross, *Density Functional Theory*, Springer, Berlin, 1990.
4. J. P. Perdew and Y. Wang, *Phys. Rev. B*, **3**, 8800 (1986).
5. J. P. Perdew, *Phys. Rev. B*, **33**, 8822 (1986).
6. A. D. Becke, *Phys. Rev. A*, **38**, 3098 (1988).
7. C. Lee, W. Yang, and R. G. Parr, *Phys. Rev. B*, **37**, 785 (1988).
8. (a) M. Levy, *Adv. Quant. Chem.* **21**, 71 (1990); (b) L. C. Wilson and M. Levy, *Phys. Rev. B*, **41**, 12930 (1990); (c) P. M. W. Gill, B. G. Johnson, and J. A. Pople, *Int. J. Quant. Chem. Symp.*, **26**, 319 (1992); (d) M. Levy and J. P. Perdew, *Int. J. Quant. Chem.*, **49**, 539 (1994).
9. J. P. Perdew, J. A. Chevary, S. H. Vosko, K. A. Jackson, M. R. Pederson, D. J. Singh, and C. Fiolhais, *Phys. Rev. B*, **46**, 6671 (1992), and **48**, 4978 (1993).
10. E. Clementi and S. J. Charravorty, *J. Chem. Phys.*, **93**, 2591 (1990).
11. N. Oliphant and R. J. Bartlett, *J. Chem. Phys.*, **100**, 6550 (1994).
12. P. Fuentealba and A. Savin, *Chem. Phys. Lett.*, **217**, 566 (1994).
13. M. Causa and A. Zupan, *Chem. Phys. Lett.*, **220**, 145 (1994).
14. A. D. Becke, *J. Chem. Phys.*, **96**, 2155 (1992), **97**, 9173 (1992).
15. D. C. Langreth and J. P. Perdew, *Phys. Rev. B*, **15**, 2884 (1977), and references cited therein.
16. A. D. Becke, *J. Chem. Phys.*, **98**, 5648 (1993).
17. A. D. Becke, *J. Chem. Phys.*, **104**, 1040 (1996).
18. J. P. Perdew and K. Burke, *Int. J. Quant. Chem. Symp.*, **57**, 309 (1996).
19. J. P. Perdew, personal communication.
20. J. P. Perdew, In *Electronic Structure of Solids '91*, P. Ziesche and H. Eschrig, Eds., Akademie Verlag, Berlin, 1991, p. 11.
21. J. P. Perdew, K. Burke, and M. Ernzerhof, *Phys. Rev. Lett.*, **77**, 3865 (1996).
22. E. I. Proynov, A. Vela, and D. R. Salahub, *Chem. Phys. Lett.*, **230**, 419 (1994).
23. E. Engel, J. A. Chevary, L. D. Macdonald, and S. H. Vosko, *Z. Phys. D*, **23**, 7 (1992).
24. R. Van Leeuwen and D. J. Baerends, *Phys. Rev. A*, **49**, 2421 (1994).
25. J. P. Perdew and A. Zunger, *Phys. Rev. B*, **23**, 5048 (1981), and references cited therein.
26. B. G. Johnson, C. A. Gonzales, P. M. W. Gill, and J. A. Pople, *Chem. Phys. Lett.*, **221**, 100 (1994).
27. G. I. Csonka and B. G. Johnson, submitted.
28. M. A. Buijse, E. J. Baerends, and J. G. Snijders, *Phys. Rev. A*, **40**, 4190 (1989).
29. R. Van Leeuwen and E. J. Baerends, *Int. J. Quant. Chem.*, **52**, 711 (1994).
30. Y. Wang and R. Parr, *Phys. Rev. A*, **47**, 1591 (1993).
31. P. Süle, O. V. Gritsenko, Á. Nagy, and E. J. Baerends, *J. Chem. Phys.*, **103**, 10085 (1995).
32. K. Burke, J. P. Perdew, and M. Levy, *Phys. Rev. A*, **53**, 2915 (1996).
33. (a) J. Wang, Z. Shi, R. J. Boyd, and C. A. Gonzales, *J. Phys. Chem.*, **98**, 6988 (1994); (b) J. Wang, L. A. Eriksson, R. J. Boyd, Z. Shi, and B. G. Johnson, *J. Phys. Chem.*, **98**, 1844 (1994); (c) J. Wang, L. A. Eriksson, B. G. Johnson, and R. J. Boyd, *J. Phys. Chem.*, **100**, 5274 (1996); (d) J. Wang, B. G. Johnson, R. J. Boyd, and L. A. Eriksson, *J. Phys. Chem.*, **100**, 6317 (1996); (e) M. Sola, J. Mestres, R. Carbo, and M. Duran, *J. Chem. Phys.*, **104**, 66 (1996).
34. S. H. Vosko, L. Wilk, and M. Nussair, *Can. J. Phys.*, **58**, 1200 (1980).
35. M. J. Frisch, G. W. Trucks, M. Head-Gordon, P. M. W. Gill, M. W. Wong, J. B. Foresman, B. G. Johnson, H. B. Schlegel, M. A. Robb, E. S. Replogle, R. Gomperts, J. L. Andres, K. Raghavachari, J. S. Binkley, C. Gonzalez, R. L. Martin, D. J. Fox, D. J. DeFrees, J. Baker, J. J. P. Stewart, and J. A. Pople, *Gaussian-92/DFT, Revision F*, Gaussian, Inc., Pittsburgh, PA, 1993.
36. M. J. Frisch, G. W. Trucks, M. Head-Gordon, P. W. M. Gill, M. W. Wong, J. B. Foresman, B. G. Johnson, H. B. Schlegel, M. A. Robb, E. S. Replogle, R. Gomperts, J. L. Andres, K. Raghavachari, J. S. Binkley, C. Gonzalez, R. L. Martin, D. J.

- Fox, D. J. DeFrees, J. Baker, J. J. P. Stewart, and J. A. Pople, *Gaussian 94, Revision B*, Gaussian, Inc., Pittsburgh, PA, 1995.
37. R. Krishnan, M. J. Frisch, and J. A. Pople, *J. Chem. Phys.*, **72**, 4244 (1980), and references cited therein.
38. R. Krishnan, J. S. Binkley, R. Seeger, and J. A. Pople, *J. Chem. Phys.*, **72**, 650 (1980).
39. R. W. F. Bader's laboratory, AIMPAC, McMaster University, Hamilton, ON L8S 4M1, Canada.
40. A. Zupan, K. Burke, M. Ernzerhof, and J. P. Perdew, *J. Chem. Phys.* (in press).
41. J. M. Seminario, *Int. J. Quant. Chem. Quant. Chem. Symp.*, **28**, 655 (1994).
42. M. Ernzerhof, J. P. Perdew, and K. Burke, In *Density Functional Theory I*, R. Nalewajski, Ed., Springer, Berlin, 1996.
43. R. Van Leeuwen and E. J. Baerends, *Int. J. Quant. Chem.*, **52**, 711 (1994).